Volume 12
Number 40
28 October 2021
Pages 13235–13598

Chemical Science

rsc.li/chemical-science

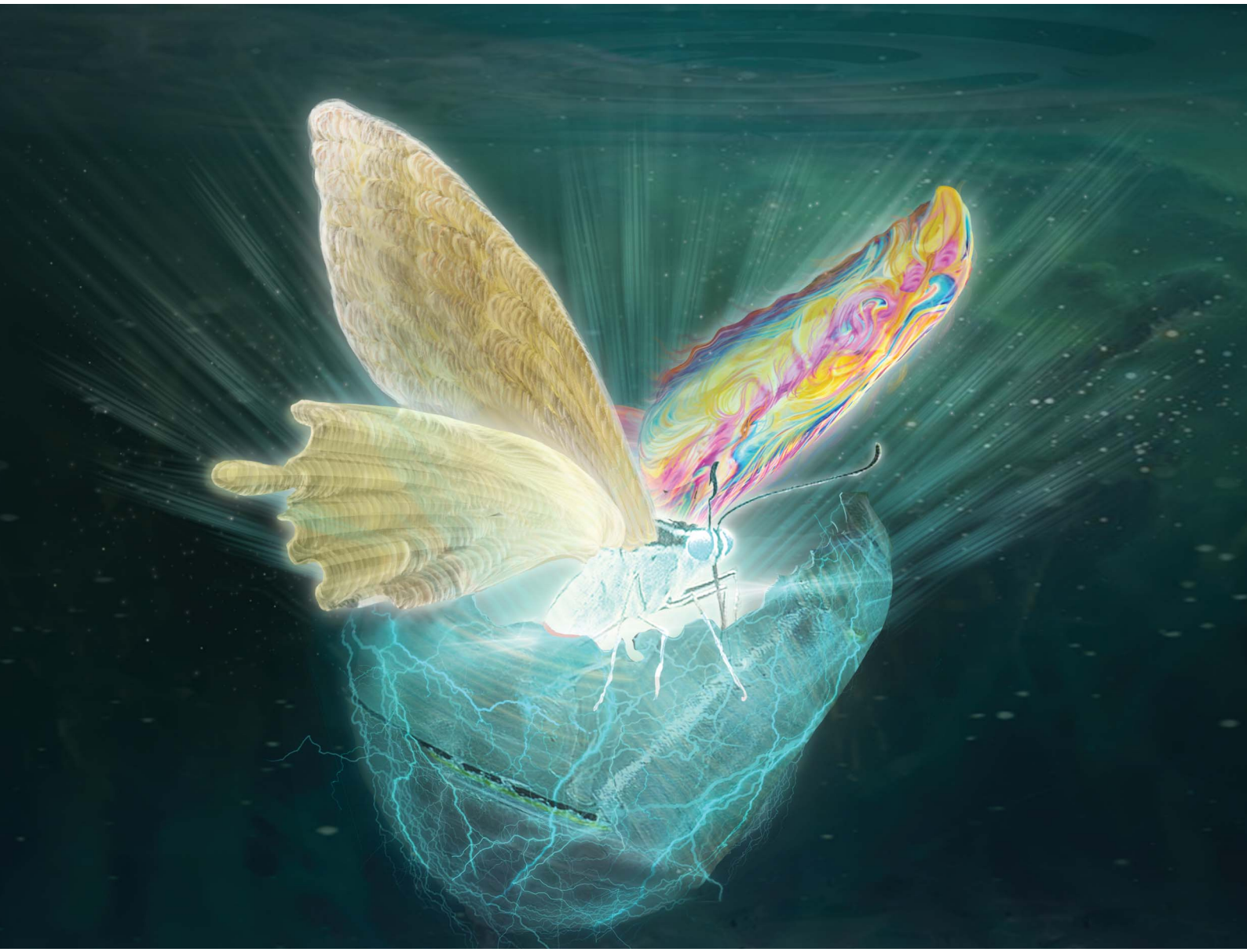

ISSN 2041-6539

ROYAL SOCIETY OF CHEMISTRY

EDGE ARTICLE

Zujin Zhao, Ben Zhong Tang, Li Niu *et al.*
Aggregation-induced delayed fluorescence luminogens: the innovation of purely organic emitters for aqueous electrochemiluminescence

Chemical Science

ROYAL SOCIETY OF CHEMISTRY

EDGE ARTICLE

View Article Online
View Journal | View Issue

Cite this: *Chem. Sci.*, 2021, **12**, 13283

All publication charges for this article have been paid for by the Royal Society of Chemistry

Received 30th May 2021
Accepted 5th September 2021

DOI: 10.1039/d1sc02918e

rsc.li/chemical-science

Aggregation-induced delayed fluorescence luminogens: the innovation of purely organic emitters for aqueous electrochemiluminescence†

Baohua Zhang, [a] Yi Kong,[a] Huijun Liu,[b] Bin Chen,[b] Bolin Zhao,[a] Yelin Luo,[a] Lijuan Chen,[a] Yuwei Zhang, [a] Dongxue Han, [a] Zujin Zhao, *[b] Ben Zhong Tang *[bc] and Li Niu *[a]

Due to overcoming the limitation of aggregation caused quenching (ACQ) of solid-state emitters, aggregation-induced emission (AIE) organic luminogens have become a promising candidate in aqueous electrochemiluminescence (ECL). However, restricted by the physical nature of fluorescence, current organic AIE luminogen-based ECL (AIECL) faces the bottleneck of low ECL efficiency. Here, we propose to construct *de novo* aqueous ECL based on aggregation-induced delayed fluorescence (AIDF) luminogens, called AIDF-ECL. Compared with the previous organic AIE luminogens, purely organic AIDF luminogens integrate the superiorities of both AIE and the utilization of dark triplets *via* thermal-activated spin up-conversion properties, thereby possessing the capability of close-to-unity exciton utilization for ECL. The results show that the ECL characteristics using AIDF luminogens are directly related to their AIDF properties. Compared with an AIECL control sample based on a tetraphenylethylene AIE moiety, the ECL efficiency of our AIDF-ECL model system is improved by 5.4 times, confirming the excellent effectiveness of this innovative strategy.

Introduction

Electrochemiluminescence (ECL),[1–5] also termed as electrogenerated chemiluminescence, is essentially related to excited state generation *via* electrochemical reaction in the vicinity of an electrode. In addition to fascinating ECL light-emitting devices[6,7] and weavable fibre applications,[8] ECL is well recognized in analytical chemistry, life and environmental sciences due to its multiple advantages as compared to chemiluminescence (CL) or photoluminescence (PL) methods, such as ultralow background signal, high sensitivity, multidimensional electrochemical regulation capability, *etc.* Very recently, aggregation-induced emission (AIE), a concept launched by Ben Zhong Tang and co-workers,[9,10] has been introduced into the ECL field as a new-generation ECL emitter.[11–19] Impressively, by using the AIE luminogens, the ubiquitous aggregation caused quenching (ACQ) issue originating from notorious π–π interactions and/or molecular-motion-induced energy dissipation has been well solved *via* the AIE effect.[10] For AIE, the water-insolubility of organic molecules is not a drawback, but actually becomes a premise and framework for constructing self-aggregated powder, film or crystalline solid-state emitters featuring much-enhanced PL quantum efficiency (Φ_{PL}). Coincidentally, this property is extremely satisfactory for the development of a qualified aqueous ECL emitter, which is the essential demand of the whole ECL technique towards various kinds of applications.[2,20]

Starting from the pioneer report on a platinum(II) complex in 2017 by De Cola's group,[11] a variety of aggregation-induced electrochemiluminescence (AIECL) emitters have emerged, such as metallic complexes,[18,21,22] metal clusters,[23] AIE organic molecules,[12,14–16,24] carbon dots[17] or polymer dots.[13,25] Meanwhile, ECL bioscience sensing studies using these emitters have also been developed, *e.g.* a chloramphenicol sensor,[26] methyltransferase assay,[27] microRNA assay[28] *etc.* However, a main challenge of the AIECL motif is the low ECL efficiency. At present, the main strategy is to improve the solid-state Φ_{PL} of AIE emitters either by chemistry or physics methods.[13–16,25] However, under electrochemical excitation, the basic charge-to-photon conversion processes that determine the ECL efficiency (Φ_{ECL}) of the AIECL system have rarely been considered.[23] It was

[a]*Centre for Advanced Analytical Science, c/o School of Chemistry and Chemical Engineering, Guangzhou University, Guangzhou Key Laboratory of Sensing Materials & Devices, Guangzhou 510006, P. R. China. E-mail: lniu@gzhu.edu.cn*

[b]*State Key Laboratory of Luminescent Materials and Devices, Guangdong Provincial Key Laboratory of Luminescence from Molecular Aggregates, South China University of Technology, Guangzhou 510640, China. E-mail: mszjzhao@scut.edu.cn; tangbenz@ust.hk*

[c]*Shenzhen Institute of Aggregate Science and Technology, School of Science and Engineering, The Chinese University of Hong Kong, Shenzhen, Guangdong 518172, China*

† Electronic supplementary information (ESI) available: Additional photophysics, electrochemical and electrochemiluminescence data and the correlated analysis. See DOI: 10.1039/d1sc02918e

noticed that, among the AIECL emitters, the reported metallic complex or cluster AIECL samples generally outperformed the others in terms of Φ_{ECL}.[11,22,23] With the assistance of the heavy-atom effect from Au, Ru or Ir metals, these AIECL systems correspond to phosphorescence in photophysics. Under electrochemical excitation, all of the generated excited states (R*) (under spin statistics,[29] the R* ratios between the lowest singlets (S_1) and triplets (T_1) in nature are close to 25%/75%) were radiatively decayed *via* a phosphorescent route. By contrast, without exception, the Φ_{ECL} behaviours of all of the purely organic AIECL emitters[12–16,25,30] were limited by their fluorescence properties. Despite the high Φ_{PL} achieved in the aggregated state, it was only the singlet excited states (^{1}R*) (~25% in total) that were harvested for ECL *via* the fluorescent route under electrochemical excitation, while the dominant triplet excited states (^{3}R*) (~75% in total) were wasted *via* a non-radiative decay channel. Previously, Ishimatsu *et al.* reported efficient ECL of donor–acceptor molecules with thermally activated delayed fluorescence (TADF) properties.[31] Owing to the small S_1/T_1 energy gap (ΔE_{ST}) and high reverse intersystem crossing (RISC) efficiency (Φ_{RISC}), the process of spin up-conversion from the T_1 to S_1 ensured the utilization of triplets generated by electrochemical excitation. In dichloromethane (DCM) medium, such TADF-type ECL renders a high Φ_{ECL} at about 50%, which was comparable to its Φ_{PL} in DCM solution. Accordingly, it is reliable to construct efficient ECL of purely organic systems to break the rules of spin statistics. Unfortunately, owing to the water-insolubility and ACQ effects of these TADF emitters,[31,32] such a mechanism is invalid in an aqueous medium. For aqueous ECL using purely organic luminophores, organic luminophores simultaneous possessing AIE and spin up-conversion properties are an ideal candidate. However, there have been no such reports so far.

Herein, we report that aggregation-induced delayed fluorescence (AIDF) luminogens[33,34] have great potential to develop efficient and stable aqueous ECL. We called this new system AIDF-ECL as this phenomenon is intrinsically based on the AIDF properties of this kind of luminogen. Considering its combination of the merits of AIE and TADF features, AIDF-ECL will be an ideal system to build aqueous ECL using purely organic luminophores. Surprisingly, a lot of efficient AIDF luminogens with different colours have been successfully explored for organic light-emitting diodes (OLEDs),[33–36] while their superiorities of AIDF properties in an aqueous medium suitable for aqueous ECL have not been considered. To our best knowledge, this work is the first attempt. As a proof of concept, we selected one AIDF luminogen and presented the direct correlation between its AIDF property and its ECL behaviours. One tetraphenylethylene (TPE)-moiety-containing AIE luminogen without AIDF properties was used as a control sample, which represents all ever-reported purely organic AIECL systems[12–16,22,24,30] that possess traditional fluorescence properties. Importantly, with a similar Φ_{PL}, the AIDF luminogen displayed an obvious enhancement in Φ_{ECL} with respect to that of the control AIE luminogen sample. Our results provide important clues for the further development and application of this new class of aqueous ECL luminophore.

Experimental section

Materials

All the chemicals and reagents were purchased from commercial sources and used as received without further purification. Ultrapure fresh water was obtained from a water purification system (>18.2 MΩ). Potassium chloride (KCl), potassium hydrogen phosphate (KH_2PO_4) and dipotassium phosphate (K_2HPO_4) were purchased from Sinopharm Chemical Reagent Co. Ltd (Shanghai, China). Acetonitrile (ACN, anhydrous, 99.8%) and tetrahydrofuran (THF, ≥99.9%) were purchased from Sigma-Aldrich Co. Ltd (Shanghai, China). Tripropylamine (TPrA, ≥98%) was purchased from Alfa Co. Ltd. Dichloromethane (DCM, 99.9%) was purchased from Innochem Co. Ltd (Beijing, China). Tetra-*n*-butylammonium hexafluorophosphate ($TBAPF_6$, 98%) was purchased from Acros Co. Ltd. The AIDF-type mCP-BP-PXZ ($C_{49}H_{31}N_3O_2$) molecule and the AIE-type TPE-TAPBI ($C_{67}H_{56}N_2$) molecule were synthesized according to our previously reported paper.[36,37] All the aqueous ECL measurements used phosphate buffered solution (PBS, pH = 7.44) containing 0.1 M KCl, 0.1 M K_2HPO_4 and 0.1 M KH_2PO_4 as the electrolyte.

General characterization

For the photophysical characterization, an Edinburgh fluorescence spectrometer (FLS1000) was used, in which transient PL and steady-state PL measurements were triggered by a picosecond pulsed LED (EPLED-365) and Xe2 xenon lamp, respectively. For direct measurement of the absolute PL quantum efficiency (PLQY) of solutions or films, integrating sphere testing accessories were coupled, which were integrated with the whole FLS1000 system and controlled by the same software. Various kinds of photophysical parameters (*e.g.* shown in Tables S1–S3†) were calculated according to the previous established theory.[36,38,39] Redox electrochemistry experiments were conducted on a CHI 660B electrochemistry workstation (CH Instruments Inc). ECL measurements were carried out on a Xi'an Remex MPI-EII ECL system. Transmission Electron Microscopy (TEM) measurements were obtained with a JEOL JEM-2100F system operated at 200 kV.

The preparation of AIDF or AIE luminogen solutions

At first, we prepared the mCP-BP-PXZ or TPE-TAPBI solutions (5 mM in concentration) in THF as the mother solution for subsequent blending or dilution. The next step is to add additional THF and/or ultrapure fresh water into these mother solutions to fabricate mCP-BP-PXZ (0.1 mM) or TPE-TAPBI (0.1 mM) luminogen solutions in a THF/H_2O blend solvent with different water factions as required, i.*e.* f_w: 0–95 vol%. To prevent agglomeration or heterogeneity, the as-prepared luminogen solutions were thoroughly shaken in general, and then used for the subsequent characterization or experiments (*e.g.* modifying the GCE electrode for CV and ECL test).

The glassy carbon electrode (GCE) modification method

Prior to usage, the GCE (4 mm in diameter) was routinely polished by using 0.3 μm and 0.05 μm alumina slurry, respectively,

which was followed by successive sonication in water, ethanol and ultrapure fresh water in sequence. Then, the GCE electrode was thoroughly rinsed with ultrapure water and dried using high-purity N_2 flow. Finally, the bare GCE was dip-coated into the mCP-BP-PXZ (20 μL, 0.1 mM) or TPE-TAPBI (20 μL, 0.1 mM) luminogen solutions in THF/H_2O mixtures with different water fractions, and dried by baking it with an infrared lamp in ambient conditions to obtain the AIDF-luminogen- or AIE-luminogen-modified GCE samples.

CV and ECL measurements

The CV experiments were tested on a CHI 660B electrochemistry workstation (CH Instruments Inc). Generally, a three-electrode system (a Pt wire as a counter electrode, a Ag wire or Ag/AgCl as a reference electrode, and a GCE or AIDF-luminogen-modified GCE or AIE-luminogen-modified GCE with a diameter of 4 mm as a working electrode) was used, which was calibrated by using a ferrocene (Fc)/ferrocenium (Fc^+) couple. CVs of mCP-BP-PXZ or TPE-TAPBI in solution (1 mM) were tested in waterless dichloromethane (DCM) (for the anode scan) or acetonitrile (ACN) (for the cathode scan) with 0.1 M $TBAPF_6$ as a supporting electrolyte under a nitrogen-filled glovebox environment and scan rate of 0.1 V s^{-1}.

Electrochemiluminescence (ECL) was tested on a MPI-EII electrochemiluminescence (Remex Electronic Instrument Lt. Co., Xi'an, China) detection system. In all aqueous ECL measurement experiments, a three-electrode system (Pt wire as a counter electrode, Ag/AgCl (saturation KCl solution) as a reference electrode, and an AIDF-luminogen-modified or AIE-luminogen-modified GCE with a diameter of 4 mm as a working electrode) was used, and the photomultiplier tube (PMT) voltage of the ECL system was set at 850 V. In detail, the luminogen modified GCE was immersed in PBS solution containing 0.1 M KCl, 0.1 M K_2HPO_4 and 0.1 M KH_2PO_4 as the electrolyte for ECL tests. Co-reactant ECL studies were conducted using the same procedures except for additionally adding 40 mM TPrA into the PBS solution. The relative ECL efficiency of the mCP-BP-PXZ luminogen modified GCE/TPrA was calculated using the TPE-TAPBI luminogen modified GCE/TPrA as the internal standard. In detail, the relative ECL efficiencies were calculated using the following equation:[30,40]

$$\Phi^{x}_{ECL} = \Phi^{0}_{ECL}\left(\frac{\int_a^b I\,dt}{\int_a^b i\,dt}\right)_x \Big/ \left(\frac{\int_a^b I\,dt}{\int_a^b i\,dt}\right)_0$$

in which, Φ^0_{ECL} is the ECL efficiency of the TPE-TAPBI modified GCE (the pre-aggregation solution conditions: 0.1 mM, $f_w = 95\%$) in PBS solution with 40 mM TPrA, which was taken as 100% as the internal reference. I, i and x are ECL intensity, current value, and the targeted emitter, *i.e.* the mCP-BP-PXZ modified GCE (the pre-aggregation solution conditions: 0.1 mM, $f_w = 95\%$) in PBS solution with 40 mM TPrA, respectively.

Results and discussion

Photophysical properties

Organic ECL emitters, except for some peculiar cases, *e.g.* triplet–triplet annihilation (TTA)-type,[29] can be divided into three kinds according to their excited state decay dynamics (Scheme 1A), *i.e.* fluorescent type (FL-ECL),[41] AIE-ECL (*i.e.* AIECL)[14–16] and AIDF-ECL (mentioned herein). Similar to electroluminescent (EL) excitation conditions,[42–44] the produced yield of S_1/T_1 excited states under electrochemical excitation is about 25%/75% under spin statistics.[29,31] Despite the merit of the AIE effect of restraining various non-radiative (NR) routes (see the comparison between FL-ECL and AIE-ECL in Scheme 1A), the ever-explored organic AIE-ECL emitters belong to fluorescence in photophysics. Under electrochemical excitation, the dominantly generated triplet excited states (75% in total) cannot be harvested for ECL, which is limited by a distinct high ΔE_{ST} level (>0.5–1.0 eV) and thus inefficient RISC process. For the AIDF luminogens in the aggregated state, a distinctly reduced ΔE_{ST} (<0.1–0.3 eV) and the favorable AIE effect are coupled to facilitate spin up-conversion from those triplets to singlets *via* RISC, and then radiative decay *via* a delayed fluorescent (DF) route. Accordingly, the harvesting of triplets is realized through the delayed fluorescence (DF)-ECL channel (Scheme 1A, bottom). In practice, a qualified AIDF molecule, namely mCP-BP-PXZ,[36] was applied in this work (see Scheme 1C for its chemical structure) to construct this novel AIDF-ECL system. When dissolved in the good solvent tetrahydrofuran (THF), its PL emission is extremely weak. After adding poor solvent water at a high content, self-aggregation occurs *via* the AIDF effect (see dashed box shown in Scheme 1B and also the followed discussion for its physics reason), along with sharply enhanced PL emission (Scheme 1B). For the control AIE-ECL system, the fluorescent-type AIE molecule, *e.g.* TPE-TAPBI (Scheme 1C for its chemical structure),[37] was used in this work. Noticeably, the desired DF-ECL process is absent for the AIE-ECL sample (Scheme 1A, middle). The intense DF *via* a fast and efficient RISC process is the peculiar photophysical basis of the AIDF-ECL strategy to be discussed.

To begin with, we introduce the peculiar difference in AIE phenomena with or without AIDF properties. Steady-state PL (Fig. 1A and B) and transient PL (Fig. 1C and D) studies were performed on these two molecules in THF/water mixtures with different water contents (f_w: 0–95 vol%). On increasing the f_w value, the PL peak intensity is monotonically enhanced, *e.g.* increasing by 71.8-fold for mCP-BP-PXZ (f_w: 0% *vs.* 95%, Fig. 1A and its inset picture) and 8.03-fold for TPE-TAPBI (f_w: 0% *vs.* 90%, Fig. 1B and its inset picture). Apparently, there is no significant difference between the steady-state PL spectrum features and the visual discernible image characteristics, *i.e.* the PL peak, full width at half maximum (FWHM), and colours. In this sense, both of them are AIE-type luminogens. In the highly aggregated state (*e.g.* larger than 80% for f_w), physical constraint of the molecular motion action largely lowers the nonradiative decay path for S_1 to S_0 transition, which contributes to the PL enhancement as observed. In particular, a distinct difference does exist in their transient PL behaviours, which is directly measured in air conditions. For mCP-BP-PXZ with the highest f_w (*i.e.* 95% *vs.* 0%), except for a significantly enhanced prompt fluorescent (PF) quantum efficiency (Φ_{PF}) (42.1% *vs.* 5.1%), a distinctly enhanced delayed fluorescent (DF) emission component was observed, corresponding to a sharp increase in DF quantum efficiency

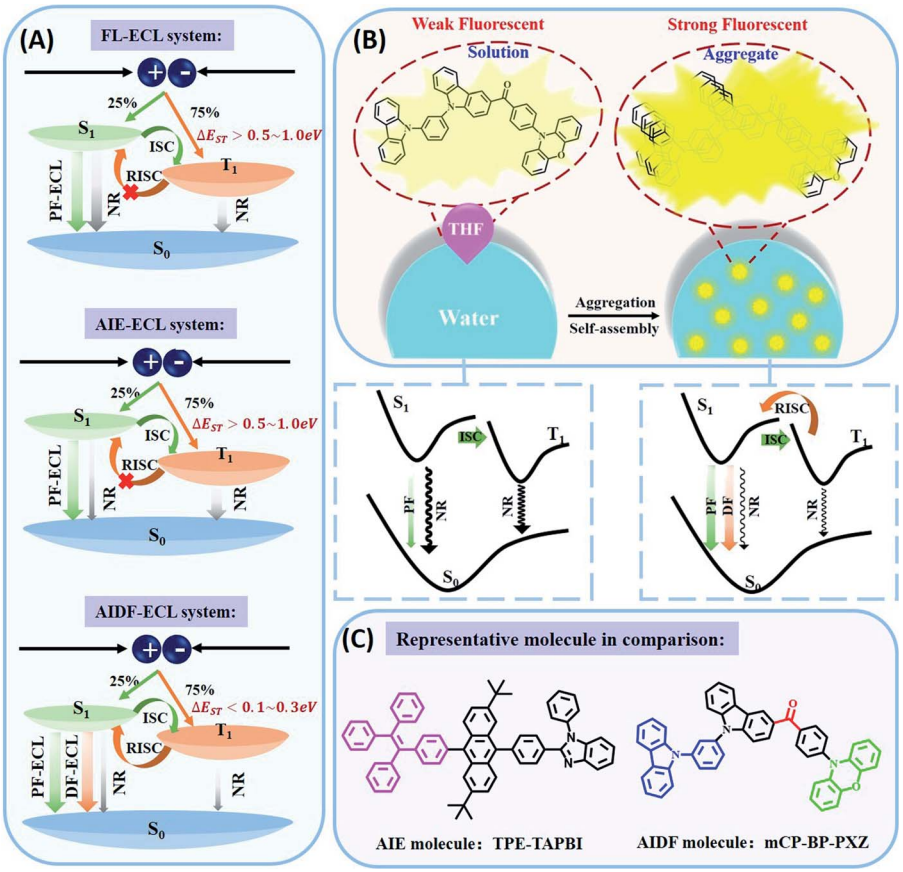

Scheme 1 (A) Schematic illustration of the fluorescent-type ECL (FL-ECL), aggregation-induced emission-type ECL (AIE-ECL) and aggregation-induced delayed fluorescence (AIDF)-type ECL (AIDF-ECL) and their mechanisms, in which S_1, T_1, S_0, PF-ECL, DF-ECL, IS, RISC and NR represent the lowest singlet state, the lowest triplet state, the ground singlet state, prompt fluorescent ECL, delayed fluorescent ECL, intersystem crossing, reverse intersystem crossing, and nonradiative deactivation, respectively. (B) Preparation of the AIDF aggregated luminogens by self-assembly in a mixed solvent. Inside the dashed box are the schematic diagrams of photophysical transitions in the molecular state in THF solution or the aggregated solid state in a THF/H_2O mixed solvent. (C) Chemical structures of AIE (left) and AIDF (right) molecules used in this report.

(Φ_{DF}) from near zero to 20.1% and a largely increased DF exciton lifetime (τ_d) to 702 ns (Fig. 1C, S1 and Table S1†). These results indicated that, with the assistance of the AIE effect, both PF originating from singlets and DF originating from triplets are feasible for mCP-BP-PXZ, which stands for a typical PL transient behaviour of AIDF luminogens.[34,36,45] As for the reasons, the enhancement in the RISC process plays the dominant role in the DF route of the mCP-BP-PXZ luminogen (dashed box shown in Scheme 1B), which is due to the unquenched S_1 (as the NR decay rate from S_1 to S_0 is largely reduced now), the small ΔE_{ST} (0.024 eV) and the enhanced spin–orbit coupling (SOC) in the aggregated condition (confirmed by theoretical calculation).[36] By contrast, irrespective of any aggregated condition for TPE-TAPBI, owing to the distinct large ΔE_{ST} (>0.3 eV), there is merely a PF contribution with ns-range exciton lifetimes (0.7 ns–2.7 ns) and no DF emission signals can be observed (Fig. 1D, S2 and Table S2†). For this kind of AIE luminogen, dark triplets cannot be harvested for radiative decay. In this respect, the photophysical characteristics of TPE-TAPBI stand for all ever-reported AIE-type organic ECL luminophores,[13–16,23–25,30] in which the harvesting issues of triplets are not considered. Due to its chemical structure, the electron cloud distribution of the highest occupied molecular orbital (HOMO) and the lowest unoccupied molecular orbital (LUMO) is highly overlapped, rendering a distinct high ΔE_{ST} and thus the blocked RISC process for DF. For mCP-BP-PXZ and its analogous, the HOMO and LUMO distribution is deliberately separated to a large extent, *e.g.* by introducing a large torsion angle with phenoxazine (PXZ) for the development of mCP-BP-PXZ.[36] As a result, both high Φ_{PL} and TADF merits are simultaneously realized for the aggregated state of the AIDF luminogens (Fig. S3 and Table S1†). Thanks to these AIDF merits, non-doped OLEDs using mCP-BP-PXZ achieved an extremely high performance, *e.g.* maximum external quantum efficiency (EQE) value at 22.1%.[36] In parallel, non-doped TPE-TAPBI-based OLEDs merely achieved a peak EQE of 5.73%.[37] Under EL excitation with spin statistics restriction, the generation ratio of singlets/triplets is also ~25%/75%. The EQE ratio of them is about 4 : 1, which implies the significance of collection of triplets for AIDF-type OLEDs.

Electrochemistry and electrochemiluminescence

For electrochemical study, glassy carbon electrodes (GCEs) were modified with such AIDF molecules by dip-coating in those

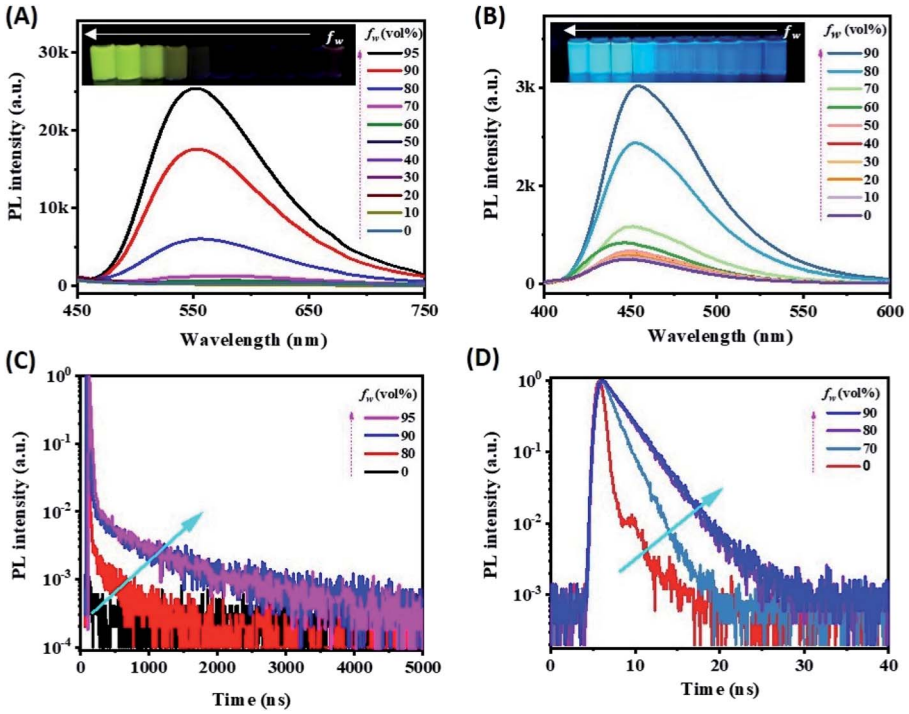

Fig. 1 PL spectra of the (A) mCP-BP-PXZ and (B) TPE-TAPBI molecule in THF/water mixtures with different water fractions (f_w). Inset: the corresponding photographs of the luminogens in THF/water mixtures under UV irradiation ($\lambda = 365$ nm). The transient PL decay curves of the (C) mCP-BP-PXZ molecule with different f_w (excitation wavelength: 363 nm, and detection wavelength: 553 nm, in air) at 300 K, and the (D) TPE-TAPBI molecule with different f_w (excitation wavelength: 363 nm, and detection wavelength: 454 nm, in air) at 300 K.

solutions and then drying at ambient conditions (see Experimental section for the details). Their photographs under UV irradiation ($\lambda = 365$ nm) (Fig. S4†) are analogous to the inset pictures shown in Fig. 1A. Similar to the solution condition (Fig. 1A), the mCP-BP-PXZ modified GCE is the brightest when the f_w is 95%. Accordingly, it is speculated that pre-aggregation occurs in the corresponding solution and directly determines the photophysical behaviour of the as-fabricated dip-coated AIDF luminogen-modified GCE. As measured by transmission electron microscopy (TEM) (Fig. S5†), the corresponding mCP-BP-PXZ dip-coated film (f_w: 95%) has the morphology of nano-aggregates, in which disk-shaped aggregates with diameters of about 50–100 nm are fused together. Under N_2 protection, its transient PL behaviours are comparable to the values measured in the solution state, *i.e.* τ_p/τ_d: 19/877 ns (Fig. S6, S7 and Table S3†), well confirming the AIDF property for the dip-coated film. As compared to the N_2-protected film sample, it is observed that the DF emission of the mCP-BP-PXZ film is lowered in air (Fig. S6†), which is due to the triplet quenching of oxygen.[46] However, the lowered degree was significantly less than that of previous TADF emitters.[31] The exact reason is still under study. As a possible reason, firstly, the fast RISC rate (2.1×10^6 s^{-1}) in such aggregated state may play an important role, which guarantees the DF route. In addition, it may be attributed to the unique AIE properties of the mCP-BP-PXZ luminogen, in which the triplet quenching by oxygen could be inhibited by molecular conformational factors, such as the restricted molecular motion. As measured, the resultant mCP-BP-PXZ dip-coated film in air possesses the τ_p/τ_d of 17 ns/453 ns and Φ_{PL} of 28.3%, in which Φ_{PF} and Φ_{DF} are 15.6% and 12.7%, respectively (Table S3†).

First, we tried an annihilation ECL test for the mCP-BP-PXZ-modified GCE sample. Unfortunately, no ECL was observed for it. The reason is probably limited by the stability of free radicals generated in the annihilation test conditions. It has been reported that in the ECL mode, the stable intermediate states formed by the co-reactant assist ECL luminophores to generate excitons, and then produce significantly enhanced ECL.[47] Herein, considering its satisfactory electrooxidation behaviour (*i.e.* a reversible and stable anodic half-wave current–potential cyclic voltammetry (CV) curve, Fig. S9†), we attempted to conduct oxidative-reduction ECL using conventional tripropylamine (TPrA)[48,49] as the co-reactant, under the conditions of a potential window of 0 V–1.3 V (*vs.*, Ag/AgCl), scan rate of 0.5 V s^{-1}, 0.1 M PBS containing 0.1 M KCl and 40 mM TPrA, and pH 7.44. As shown in Fig. 2A (taking $f_w = 95\%$ as an example), the current starts to rise rapidly from about 0.74 V, while the ECL signal does not start to rise until after 0.97 V, and then reaches the peak value at 1.28 V (Fig. 2B). For the bare GCE containing TPrA alone in the electrolytic cell, extremely weak ECL is produced (Fig. S10†). For the AIDF-luminogen-modified GCE, ECL was also not observed in the absence of TPrA (not shown here). Therefore, the corresponding emission mechanism should be a TPrA-involved co-reactant ECL mode.[15,25] In detail, during the electrooxidation process, the AIDF luminogens (AIDF gen) are first oxidized to generate cationic radicals on the

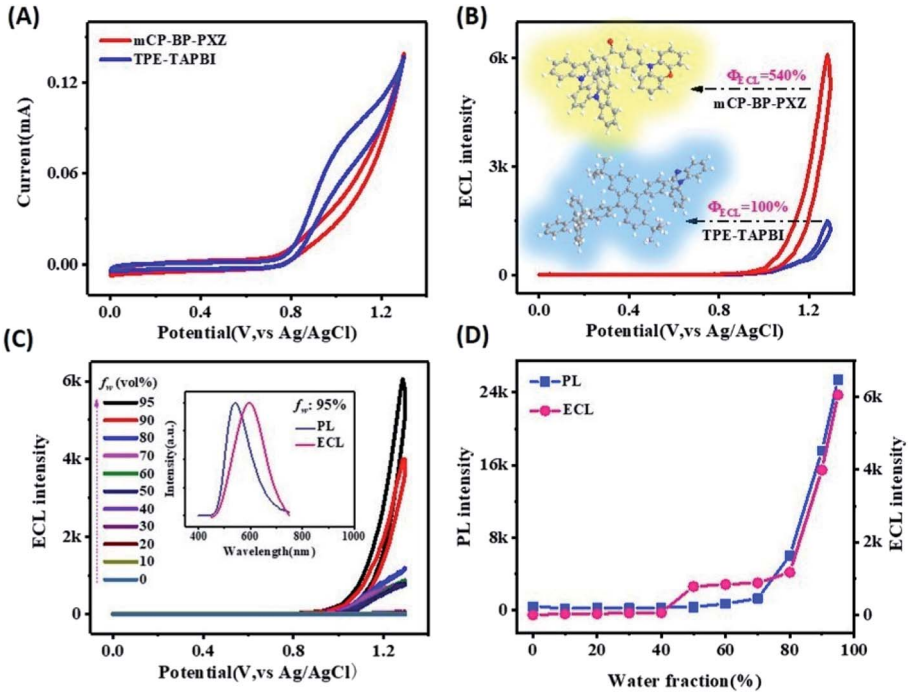

Fig. 2 (A) Anodic cyclic voltammograms and (B) the oxidative-reduction ECL responses of the AIDF molecule (red line, f_w: 95%) and AIE molecule (blue line, f_w: 95%). (C) The oxidative-reduction ECL responses of the AIDF luminogen-modified GCE under the conditions of a potential window ranging from 0 V to 1.3 V (*vs.* Ag/AgCl), scan rate of 0.5 V s^{-1}, 0.1 M PBS containing 0.1 M KCl and 40 mM TPrA, and pH 7.44. PMT: 850 V. Inset: PL and ECL spectrum of the AIDF luminogen in the solid state (f_w: 95%). (D) PL and ECL trends of the AIDF luminogen with different f_w.

GCE electrode (AIDF gen$^{\bullet+}$). On further increasing the oxidation potential, TPrA molecules are oxidized to produce a sufficient amount of strong reductive intermediates, *i.e.* TPrA$^{\bullet}$, so as to collide with the AIDF gen$^{\bullet+}$ to generate excitons on mCP-BP-PXZ (AIDF gen*), and then produce ECL (Fig. 3A). As for the ECL spectrum (inset graph in Fig. 2C), the emission peak (596 nm) displayed a 53 nm redshift with respect to its PL spectrum (543 nm). The exact reason is still unclear. To understand it, we noticed that a similar distinct redshift phenomenon was also observed for the AIECL of carboranyl carbazole nanoaggregates in the aggregated state.[16] As suggested, in view of the morphology-related ECL spectra, the surface state transition may be involved, which is analogous to the well-known redshift phenomena typically occurring in semiconductor nanomaterial ECL emitters.[50]

At the same time, we observed that the ECL intensity increased with the increase of water content f_w (0–95%) of the AIDF luminogens that were dispersed for pre-aggregation. The reason can be mainly attributed to two aspects as we observed: (i) the oxidation current was gradually increased on increasing the f_w (Fig. S10†). Therefore, under the same potential, it is likely that more free AIDF radical cations (AIDF gen$^{\bullet+}$) are generated, which could collide with the reductive intermediates of TPrA (TPrA$^{\bullet}$) to generate more excitons (AIDF gen*, either singlets (25% in total) or triplets (75% in total) in excitonic nature), and then radiative decay *via* ECL. On increasing the water fraction (f_w) of the mCP-BP-PXZ solution, intermolecular arrangement of AIDF luminogens in the solid state might be enhanced, which would promote the charge transport properties of the mCP-BP-PXZ-modified GCE working electrode. (ii) The exciton radiative decay efficiency of the mCP-BP-PXZ-modified GCE electrode increases with the increase of f_w. As shown in Fig. 2C and D, the variation trend of the ECL intensity is basically consistent with that of the PL intensity of the corresponding mCP-BP-PXZ luminogens. Since the AIDF effect of mCP-BP-PXZ luminogens is monotonically enhanced on increasing the f_w (Fig. 1A and C), the achieved ECL intensity–potential behaviours of the AIDF sample shown in Fig. 2C are reasonable, which is an intrinsic characteristic of the AIDF-ECL scaffold.

As for evaluating of ECL efficiency, it is difficult to make direct comparisons between our solid-state AIDF luminogen-modified GCE/TPrA and the standard liquid-phase $Ru(bpy)_3^{2+}$/TPrA reference, since they have different concentrations of ECL emitters, and different dynamic factors, such as radical/ion diffusion and migration rate. To confirm the effectiveness of the AIDF property on the ECL efficiency of AIE-type luminogens, a TPE-TAPBI-modified GCE was used as the control condition (Fig. S11†), since it was confirmed to be an AIE luminogen without AIDF properties (mentioned above). As shown in Fig. 2A and B, we compared the behaviours of CV and co-reactant ECL for the mCP-BP-PXZ and TPE-TAPBI luminogens in the same preparation conditions. Using a routinely relative ECL efficiency calculating method (see Experimental section)[30,40] and taking the ECL efficiency of the TPE-TAPBI-modified GCE/TPrA sample as a reference (set as 100%), the relative ECL efficiency of our AIDF-ECL sample is calculated as 540%. The electrochemical currents of the two systems are basically comparable (Fig. 2A

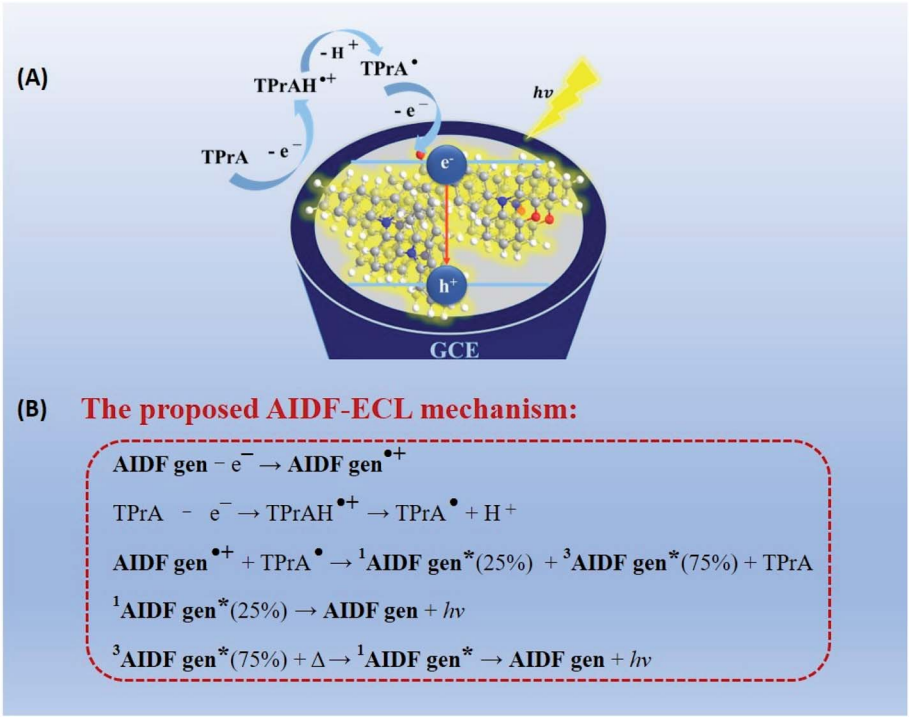

Fig. 3 (A) The schematic subprocesses of oxidative-reduction ECL of the AIDF-luminogen-modified GCE/TPrA couple and (B) the proposed ECL mechanisms, in which 1AIDF gen* and 3AIDF gen* represent singlet and triplet excited states that were electrochemically generated on AIDF luminogens, respectively.

and Table S5†). The content of co-reactant TPrA is also the same (40 mM), so its effect on the electrochemical current is also similar. Therefore, the number of cationic radicals and intermediates of TPrA produced by such oxidative-reduction ECL mode should be comparable. The difference in relative ECL efficiency thus mainly comes from the difference in ECL intensity. Although the Φ_{PL} values of the two samples are similar (28.3% and 34.0%, measured in air) (Table S6†), the ECL efficiency of the AIDF-ECL sample is greatly improved considering that AIDF samples can effectively utilize triplet excitons generated by electrochemical excitation. Possible ECL mechanisms of AIDF luminogens are thus schematically listed in Fig. 3B. On the basis of the AIE framework, it is shown that AIDF-ECL has a significant superiority for aqueous ECL with much higher efficiency. Under electrochemical excitation, it not only inhibits ACQ in an aqueous medium *via* self-aggregation, but the AIDF property means that it has the intrinsic capability to fully utilize singlet and triplet excitons for radiative decay during the ECL test.

Finally, we also briefly evaluated the stability of AIDF luminogens for aqueous ECL test conditions. Through 50 cycles of stability tests, we found that under good AIDF pre-aggregation conditions (*e.g.* f_w: 95%–80%), the ECL intensity of mCP-BP-PXZ luminogens is basically not changed (Fig. S12 and S13†). Also, at a wide concentration range of TPrA from 80 mM to 200 mM for real sensing applications, the ECL stability is also excellent (Fig. S14†). This indicates that the ECL decay dynamic behaviours of AIDF luminogens are stable under aqueous electrochemical conditions. AIDF luminogens, *e.g.* mCP-BP-PXZ used herein, were qualified as a potential candidate for efficient, reliable and reversible ECL.

Conclusions

In conclusion, an innovation within the AIECL topic is described. Compared with all of the developed AIECL organic luminophores, the model molecule that we studied has unique AIDF photophysical characteristics, namely the synergism of AIE characteristics and triplet-to-singlet spin up-conversion by thermal activation. Using one conventional AIECL model emitter (*i.e.* TPE-TAPBI) as a control, the ECL efficiency is improved by 5.4 times by using one AIDF-ECL model emitter (*i.e.* mCP-BP-PXZ), while both of them have similar PL efficiency (Φ_{PL}: 34.0% *vs.* 28.3%). This demonstrates the great potential of AIDF organic luminogens in achieving much higher aqueous ECL efficiency as compared to the earlier suggested AIE organic luminogen analogues. However, ECL study in aqueous media using AIDF luminogens is still in its infancy. The next step will be to focus on further disclosing the related mechanisms in-depth, so as to accelerate its development in the fascinating ECL field.

Data availability

Supporting data for this article have been uploaded as part of the ESI† material.

Author contributions

B.-H. Zhang and L. Niu conceived the idea. B.-H. Zhang designed the experiments and wrote the manuscript. Z.-J. Zhao and B.-Z. Tang designed the synthesis of the AIE materials. H.-J. Liu and B. Chen synthesized the AIE materials. Y. Kong performed the corresponding photophysical, electrochemistry and electrochemiluminescence experiments. B.-L. Zhao, Y.-L. Luo, L.-J. Chen, Y.-W. Zhang and D.-X. Han assisted with the data collection and analysis. B.-H. Zhang, Z.-J. Zhao and Y. Kong assisted with the manuscript revision.

Conflicts of interest

There are no conflicts to declare.

Acknowledgements

This work was supported by the foundations from the Research & Development Projects in Key Areas of Guangdong Province, China (2019B010933001), the National Natural Science Foundation of China (51773195), the Natural Science Foundation of Guangdong Province (2019B030301003, 2021A1515010510, 2021B1515020048) and Guangzhou Science and Technology Plan Project (202102010409, 202102010390, 202102010487). We highly appreciate Miss S.X. Song for her professional CV test and data analysis during the revision stage of this work.

Notes and references

1 M. M. Richter, *Chem. Rev.*, 2004, **104**, 3003–3036.
2 W. J. Miao, *Chem. Rev.*, 2008, **108**, 2506–2553.
3 A. Fiorani, G. Valenti, M. Iurlo, M. Marcaccio and F. Paolucci, *Curr. Opin. Electrochem.*, 2018, **8**, 31–38.
4 Y. Q. Chen, S. Quan, F. X. Du, B. H. Lou, J. P. Li and G. B. Xu, *Chin. J. Anal. Chem.*, 2021, **49**, 849–857.
5 X. Ma, W. Gao, F. Du, F. Yuan, J. Yu, Y. Guan, N. Sojic and G. Xu, *Acc. Chem. Res.*, 2021, **54**, 2936–2945.
6 S. Lee, H. J. Lee, Y. Ji, K. H. Lee and K. Hong, *Adv. Mater.*, 2021, **33**, 2005456.
7 K. Schlingman, Y. Chen, R. S. Carmichael and T. B. Carmichael, *Adv. Mater.*, 2021, **33**, 2006863.
8 Z. T. Zhang, K. P. Guo, Y. M. Li, X. Y. Li, G. Z. Guan, H. P. Li, Y. F. Luo, F. Y. Zhao, Q. Zhang, B. Wei, Q. B. Pei and H. S. Peng, *Nat. Photonics*, 2015, **9**, 233–238.
9 J. D. Luo, Z. L. Xie, J. W. Y. Lam, L. Cheng, H. Y. Chen, C. F. Qiu, H. S. Kwok, X. W. Zhan, Y. Q. Liu, D. B. Zhu and B. Z. Tang, *Chem. Commun.*, 2001, 1740–1741.
10 J. Mei, N. L. C. Leung, R. T. K. Kwok, J. W. Y. Lam and B. Z. Tang, *Chem. Rev.*, 2015, **115**, 11718–11940.
11 S. Carrara, A. Aliprandi, C. F. Hogan and L. De Cola, *J. Am. Chem. Soc.*, 2017, **139**, 14605–14610.
12 H. W. Liu, L. F. Wang, H. F. Gao, H. L. Qi, Q. Gao and C. X. Zhang, *ACS Appl. Mater. Interfaces*, 2017, **9**, 44324–44331.
13 Z. Wang, Y. Feng, N. Wang, Y. Cheng, Y. Quan and H. Ju, *J. Phys. Chem. Lett.*, 2018, **9**, 5296–5302.
14 Z. Han, Z. Yang, H. Sun, Y. Xu, X. Ma, D. Shan, J. Chen, S. Huo, Z. Zhang, P. Du and X. Lu, *Angew. Chem., Int. Ed.*, 2019, **58**, 5915–5919.
15 J. L. Liu, J. Q. Zhang, Z. L. Tang, Y. Zhuo, Y. Q. Chai and R. Yuan, *Chem. Sci.*, 2019, **10**, 4497–4501.
16 X. Wei, M.-J. Zhu, Z. Cheng, M. Lee, H. Yan, C. Lu and J.-J. Xu, *Angew. Chem., Int. Ed.*, 2019, **58**, 3162–3166.
17 J. R. Adsetts, S. Hoesterey, C. Gao, D. A. Love and Z. Ding, *Langmuir*, 2020, **36**, 14432–14442.
18 L. P. Lu, L. L. Zhang, W. J. Miao, X. Y. Wang and G. S. Guo, *Anal. Chem.*, 2020, **92**, 9613–9619.
19 Z. Wang, J. Pan, Q. Li, Y. Zhou, S. Yang, J.-J. Xu and D. Hua, *Adv. Funct. Mater.*, 2020, **30**, 2000220.
20 W. Lv, H. Ye, Z. Yuan, X. Liu, X. Chen and W. Yang, *TrAC, Trends Anal. Chem.*, 2020, **123**, 115767.
21 S. Carrara, B. Stringer, A. Shokouhi, P. Ramkissoon, J. Agugiaro, D. J. D. Wilson, P. J. Barnard and C. F. Hogan, *ACS Appl. Mater. Interfaces*, 2018, **10**, 37251–37257.
22 H. Gao, N. Zhang, Y. Li, W. Zhao, Y. W. Quan, Y. X. Cheng, H. Y. Chen and J. J. Xu, *Sci. China: Chem.*, 2020, **63**, 715–721.
23 H. P. Peng, Z. N. Huang, H. H. Deng, W. H. Wu, K. Y. Huang, Z. L. Li, W. Chen and J. W. Liu, *Angew. Chem., Int. Ed.*, 2020, **59**, 9982–9985.
24 Y. Zhang, Y. Zhao, Z. Han, R. Zhang, P. Du, Y. Wu and X. Lu, *Angew. Chem., Int. Ed.*, 2020, **59**, 23261–23267.
25 S. Y. Ji, W. Zhao, H. Gao, J. B. Pan, C. H. Xu, Y. W. Quan, J. J. Xu and H. Y. Chen, *iScience*, 2020, **23**, 100774.
26 S. Li, X. Ma, C. Pang, M. Wang, G. Yin, Z. Xu, J. Li and J. Luo, *Biosens. Bioelectron.*, 2021, **176**, 112944.
27 L. Cui, M.-H. Zhao, C.-C. Li, Q. Wang, X. Luo and C.-Y. Zhang, *Anal. Chem.*, 2021, **93**, 2974–2981.
28 J. L. Liu, Y. Zhuo, Y. Q. Chai and R. Yuan, *Chem. Commun.*, 2019, **55**, 9959–9962.
29 A. J. Bard, *Electrogenerated Chemiluminescence*, Marcel Dekker, Inc., 2004.
30 L. Cui, S. Yu, W. Gao, X. Zhang, S. Deng and C.-Y. Zhang, *ACS Appl. Mater. Interfaces*, 2020, **12**, 7966–7973.
31 R. Ishimatsu, S. Matsunami, T. Kasahara, J. Mizuno, T. Edura, C. Adachi, K. Nakano and T. Imato, *Angew. Chem., Int. Ed.*, 2014, **53**, 6993–6996.
32 P. Huang, B. Zhang, Q. Hu, B. Zhao, Y. Zhu, Y. Zhang, Y. Kong, Z. Zeng, Y. Bao, W. Wang, Y. Cheng and L. Niu, *ChemPhysChem*, 2021, **22**, 726–732.
33 J. J. Guo, Z. J. Zhao and B. Z. Tang, *Adv. Opt. Mater.*, 2018, **6**, 1800264.
34 R. Furue, T. Nishimoto, I. S. Park, J. Lee and T. Yasuda, *Angew. Chem., Int. Ed.*, 2016, **55**, 7171–7175.
35 H. J. Kim, M. Godumala, S. K. Kim, J. Yoon, C. Y. Kim, H. Park, J. H. Kwon, M. J. Cho and D. H. Choi, *Adv. Opt. Mater.*, 2020, **8**, 1902175.
36 H. J. Liu, J. J. Zeng, J. J. Guo, H. Nie, Z. J. Zhao and B. Z. Tang, *Angew. Chem., Int. Ed.*, 2018, **57**, 9290–9294.
37 B. Chen, B. Q. Liu, J. J. Zeng, H. Nie, Y. Xiong, J. H. Zou, H. L. Ning, Z. M. Wang, Z. J. Zhao and B. Z. Tang, *Adv. Funct. Mater.*, 2018, **28**, 1803369.
38 Y. Tao, K. Yuan, T. Chen, P. Xu, H. Li, R. Chen, C. Zheng, L. Zhang and W. Huang, *Adv. Mater.*, 2014, **26**, 7931–7958.

39 X. Lin, Y. Zhu, B. Zhang, X. Zhao, B. Yao, Y. Cheng, Z. Li, Y. Qu and Z. Xie, *ACS Appl. Mater. Interfaces*, 2018, **10**, 47–52.
40 F. Wang, J. Lin, T. Zhao, D. Hu, T. Wu and Y. Liu, *J. Am. Chem. Soc.*, 2016, **138**, 7718–7724.
41 H. Qi, C. Zhang, Z. Huang, L. Wang, W. Wang and A. J. Bard, *J. Am. Chem. Soc.*, 2016, **138**, 1947–1954.
42 S. Wang, H. Zhang, B. Zhang, Z. Xie and W.-Y. Wong, *Mater. Sci. Eng., R*, 2020, **140**, 100547.
43 M. A. Baldo, D. F. O'Brien, M. E. Thompson and S. R. Forrest, *Phys. Rev. B*, 1999, **60**, 14422–14428.
44 D. F. O. B. M. A. Baldo, Y. You, A. Shoustikov, M. E. T. S. Sibley and S. R. Forrest, *Nature*, 1998, **395**, 151.
45 J. Huang, H. Nie, J. Zeng, Z. Zhuang, S. Gan, Y. Cai, J. Guo, S.-J. Su, Z. Zhao and B. Z. Tang, *Angew. Chem., Int. Ed.*, 2017, **56**, 12971–12976.
46 R. Ishimatsu, Y. Kirino, C. Adachi, K. Nakano and T. Imato, *Chem. Lett.*, 2016, **45**, 1183–1185.
47 A. Zanut, A. Fiorani, S. Canola, T. Saito, N. Ziebart, S. Rapino, S. Rebeccani, A. Barbon, T. Irie, H. P. Josel, F. Negri, M. Marcaccio, M. Windfuhr, K. Imai, G. Valenti and F. Paolucci, *Nat. Commun.*, 2020, **11**, 2668.
48 Q. Li, J. Y. Zheng, Y. L. Yan, Y. S. Zhao and J. N. Yao, *Adv. Mater.*, 2012, **24**, 4745–4749.
49 L. Wu, J. S. Wang, L. Y. Feng, J. S. Ren, W. L. Wei and X. G. Qu, *Adv. Mater.*, 2012, **24**, 2447–2452.
50 P. Wu, X. Hou, J.-J. Xu and H.-Y. Chen, *Chem. Rev.*, 2014, **114**, 11027–11059.